THE JOURNAL OF BIOLOGICAL CHEMISTRY VOL. 290, NO. 17, pp. 11119–11129, April 24, 2015

RhoGDIβ Inhibits Bone Morphogenetic Protein 4 (BMP4)-induced Adipocyte Lineage Commitment and Favors Smooth Muscle-like Cell Differentiation*

Received for publication, August 29, 2014, and in revised form, March 15, 2015 Published, JBC Papers in Press, March 16, 2015, DOI 10.1074/jbc.M114.608075

Hai-Yan Huang[‡1,2], Wen-Ting Zhang[‡1], Wen-Yan Jiang[‡], Su-Zhen Chen[‡], Yang Liu[‡], Xin Ge[‡], Xi Li[‡], Yong-Jun Dang[‡], Bo Wen[‡], Xiao-Hui Liu[§], Hao-Jie Lu[§], and Qi-Qun Tang[‡3]

From the [‡]Key Laboratory of Metabolism and Molecular Medicine, the Ministry of Education, Department of Biochemistry and Molecular Biology, Fudan University Shanghai Medical College, Shanghai 200032 and the [§]Institutes of Biomedical Sciences, Fudan University, Shanghai 200032, People's Republic of China

Background: Bone morphogenetic protein 4 (BMP4) can induce C3H10T1/2 mesenchymal stem cell commitment into the adipocyte lineage.
Results: Overexpression of RhoGDIβ in C3H10T1/2 cells prevented BMP4-induced adipogenic commitment, whereas it facilitated expression of smooth muscle-like cell-specific markers.
Conclusion: RhoGDIβ plays opposing roles in committing C3H10T1/2 cells to adipocytes and smooth muscle-like cells.
Significance: This is a first report implicating a role of RhoGDIβ in C3H10T1/2 cells fate decisions.

The integration of signals involved in deciding the fate of mesenchymal stem cells is largely unknown. We used proteomics profiling to identify RhoGDIβ, an inhibitor of the small G-protein Rho family, as a component that regulates commitment of C3H10T1/2 mesenchymal stem cells to the adipocyte or smooth muscle cell lineage in response to bone morphogenetic protein 4 (BMP4). RhoGDIβ is notably down-regulated during BMP4-induced adipocytic lineage commitment of C3H10T1/2 mesenchymal stem cells, and this involves the cytoskeleton-associated protein lysyl oxidase. Excess RhoGDIβ completely prevents BMP4-induced commitment to the adipocyte lineage and simultaneously stimulates smooth muscle cell commitment by suppressing the activation of Rac1. Overexpression of RhoGDIβ induces stress fibers of F-actin by a process involving phosphomyosin light chain, indicating that cytoskeletal tension regulated by RhoGDIβ contributes to determining adipocyte *versus* myocyte commitment. Furthermore, the overexpression of RacV12 (constitutively active form of Rac1) totally rescues the inhibition of adipocyte commitment by RhoGDIβ, simultaneously preventing formation of the smooth muscle-like phenotype and disrupting the stress fibers in cells overexpressing RhoGDIβ. Collectively, these results indicate that RhoGDIβ functions as a novel BMP4 signaling target that regulates adipogenesis and myogensis.

Obesity is characterized by an expansion of fat mass through adipocyte hypertrophy and hyperplasia (1–4). The increase in adipocyte number is mainly due to the recruitment and commitment of mesenchymal stem cells (MSCs)[4] and subsequent terminal differentiation (5–9). Under different inducing conditions, MSCs can differentiate into multiple mesoderm cell types, including myoblasts, osteoblasts, and chondrocytes as well as adipocytes (10–12).

The C3H10T1/2 cell line, derived from C3H mouse embryos (13), behaves similarly to mesenchymal stem cells (14). BMP4 (bone morphogenetic protein 4) induces nearly complete commitment of C3H10T1/2 cells to the adipocyte lineage (15–18). However, C3H10T1/2 cells can also undergo commitment toward smooth muscle cells (SMCs) under different inducing conditions (19–21), suggesting that adipocytes and SMCs share a common mesenchymal origin. Indeed, recent research has demonstrated that a subset of beige adipocytes has a smooth muscle-like origin, and vascular smooth muscle cells can be converted into UCP1-positive adipocytes via ectopic expression of PRDM16 (22). These data indicate the possibility of a direct cell fate switch between adipocytes and SMCs.

Several studies have noted that changes in cell shape and cytoskeletal tension can influence the fate of mesenchymal progenitor cells (23, 24). We recently reported that three cytoskeleton-associated proteins including Lox (lysyl oxidase) were remarkably up-regulated concomitantly with notable F-actin (filamentous actin) disruption during BMP4-induced adipocyte lineage commitment (15–18). Knockdown of Lox reorganized the F-actin into stress fibers and totally inhibited commitment to the adipocyte lineage, suggesting that a Lox-mediated cytoskeleton change is indispensable for such com-

* This work was supported in part by National Key Basic Research Project Grant 2011CB910201, the State Key Program of National Natural Science Foundation Grant 31030048C120114, and National Natural Science Foundation Grant 81390350 (to Q. Q. T.) and Grants 31271489 and 81170781 (to H. H.). The Department of Biochemistry is supported by Shanghai Leading Academic Discipline Project, Project number B110.
[1] Both authors contributed equally to this paper.
[2] To whom correspondence may be addressed: Key Laboratory of Metabolism and Molecular Medicine, Ministry of Education, and Department of Biochemistry and Molecular Biology, Fudan University Shanghai Medical College, Shanghai 200032, China. Tel.: 01186-21-54237198; Fax: 01186-21-54237290; E-mail: haiyanhuang@shmu.edu.cn.
[3] To whom correspondence may be addressed. E-mail: qqtang@shmu.edu.cn.

[4] The abbreviations used are: MSC, mesenchymal stem cell; BMP4, bone morphogenetic protein 4; SMC, smooth muscle cell; Lox, lysyl oxidase; GDI, GDP dissociation inhibitors; TRITC, tetramethylrhodamine isothiocyanate; PAK, p21-activated kinase; PBD, protein-binding domain.

mitment under the influence of BMP4 (15). Interestingly, changes in cytoskeletal tension can also regulate SMC differentiation. It has been demonstrated that inhibition of actin polymerization significantly decreased the expression of SMC differentiation marker genes. In contrast, increased actin polymerization improved the expression of those genes (25). Because inhibition of Lox promotes actin stress fiber formation (15, 26), we hypothesized that Lox regulates adipocyte and SMC fates via regulation of actin filament formation.

Rho GTPases (Rho, Rac, and Cdc42) are known to regulate the assembly and organization of F-actin in response to extracellular cues (27–30). The RhoGDIs (Rho GDP dissociation inhibitors) inhibit the dissociation of GDP from Rho and GTP hydrolysis on Rho proteins (31). The mammalian RhoGDI family has three members: RhoGDIα, RhoGDIβ, and RhoGDIγ. The Rho GDP dissociation inhibitor β gene is commonly referred to as ARHGDIB, but is also known as LyGDI, GDI-D4, RhoGDI2, or RhoGDIβ. In this study, using iTRAQ-based proteomics profiling, we indentify RhoGDIβ as a potential target of the BMP4-Lox signaling axis, regulating commitment of C3H10T1/2 cells to either adipocytes or smooth muscle-like cells by reorganizing actin filament formation in a Rac1-dependent manner.

EXPERIMENTAL PROCEDURES

Cell Culture and Induction of Commitment/Differentiation—To induce lineage commitment, C3H10T1/2 stem cells were plated at low density and cultured in DMEM containing 10% calf serum without or with purified recombinant BMP4 (10 ng/ml). To induce adipocyte differentiation, 2-day post-confluent cells (day 0) were fed with DMEM containing 10% fetal bovine serum (FBS), 1 μg/ml of insulin, 1 μM dexamethasone, and 0.5 mM 3-isobutyl-1-methylxanthine for 2 days and then given DMEM with 10% FBS and 1 μg/ml of insulin for another 2 days, after which they were cultured in DMEM with 10% FBS. To induce SMC differentiation, 2-day post-confluent cells were fed with DMEM containing 2% horse serum for 7 days.

Oil Red O Staining—C3H10T1/2 stem cells were induced to adipocyte differentiation as described above. On day 8, the cells were washed three times with PBS (phosphate-buffered saline) and then fixed for 10 min with 3.7% formaldehyde. Oil Red O (0.5% in isopropyl alcohol) was diluted with water (3:2), filtered through a 0.45-μm filter, and incubated with the fixed cells for 1 h at room temperature. The cells were then washed with water and the stained fat droplets in the adipocytes were visualized by light microscopy and photographed.

Western Blotting—Cells were washed with ice-cold PBS (pH 7.4) and scraped into lysis buffer containing 50 mM Tris-HCl (pH 6.8), 2% SDS, phosphatase inhibitors (10 mM Na_3VO_4 and 10 mM NaF), and protease inhibitor mixture (Roche Applied Science). Equal amounts of protein were subjected to SDS-PAGE and immunoblotted with specific primary antibodies. Lox antibodies were from Santa Cruz Biotechnology (Santa Cruz, CA); RhoGDIβ antibodies were from Abgent (San Diego, CA); Acta2 antibodies were from Abcam (Cambridge, UK); Calponin1 antibody was from Epitomics (Burlingame, CA); Cofilin, phospho-Cofilin, MLC, and phospho-MLC antibodies were from Cell Signaling Technology (Beverly, MA); Rac1 antibodies were from BD Bioscience; β-actin antibody was from Sigma.

Construction of Expression Plasmids and Generation of Retrovirus—cDNA for RhoGDIβ was generated by PCR using the following primers: 5′-GGAAGATCTGCCACCATGACGGAGAAGGATGCA-3′ (forward); 5′-CCGGTTAACTCATTCTGTCCAATCCTTC-3′ (reverse). The PCR product was cloned into a MSCV retroviral vector with BglII and HpaI. A constitutively active mutant of Rac1 (RacV12) was provided by Dr. Debbie C. Thurmond (Indiana University School of Medicine). RacV12 cDNAs were subcloned into MSCV retroviral vectors with BglII and XhoI. 293T cells cultured in serum-free DMEM were transfected with MSCV or recombinant plasmid and Ecopac plasmids at 95% confluence. Fresh medium containing 10% calf serum was given 4–6 h after transfection and the viral medium was collected at 48–72 h. C3H10T1/2 cells were infected with viruses at 20–30% confluence with Polybrene (8 μg/ml).

Real-time Quantitative PCR—Total RNA was isolated using TRIzol reagent (Invitrogen). PrimeScript RT Master Mix (TaKaRa) was used for first strand cDNA synthesis with random primers. Real-time quantitative PCRs were carried out with 2× PCR Master Mix (Power SYBR Green; Applied Biosystems, Foster City, CA) on an Applied Biosystems 7300 Real-time PCR System (Applied Biosystems). Primers were as follows: 18 S rRNA, 5′-CGGCTACCACATCCAAGGAA-3′ (forward) and 5′-GCTGGAATTACC GCGGCT-3′ (reverse); *Acta2*, 5′-GTCCCAGACATCAGGGAGTAA-3′ (forward) and 5′-TCGGAT ACTTCAGCGTCAGGA-3′ (reverse); *Calponin1*, 5′-AAACAAGAGCGGAGATTTGAGC-3′ (forward) and 5′-TGTCGCAGTGTTCCATGCC-3′ (reverse); *Sm22α*, 5′-CAACAAGGGTCCATCCTACGG-3′ (forward) and 5′-ATCTGGGCGGCCTACATCA-3′ (reverse); *Sm22β*, 5′-CCTGGCCGTGAGAACTTCC-3′ (forward) and 5′-GTCCGTGGTGTTAATGCCATAG-3′ (reverse); *smMHC*, 5′-AAGCTGCGGCTAGAGGTCA-3′ (forward) and 5′-CCCTCCCTTTGATGGCTGAG-3′ (reverse); *RhoGDIα*, 5′-AAGGACGATGAAAGCCTCCG-3′ (forward) and 5′-GGTCAGTCGAGTCACAATGACA-3′ (reverse); *RhoGDIβ*, 5′-ACCCAACAGTTCCCAACGTG-3′ (forward) and 5′-GAGATCGCCAGTAAGGTCCA-3′ (reverse); *RhoGDIγ*, 5′-GTCAACTCCATCAGATGAGGTG-3′ (forward) and 5′-GGGGTCCATAATGGGTGGC-3′ (reverse).

RNA Interference—Stealth siRNA duplexes specific for *Lox* were designed and synthesized by Invitrogen. The sequence for successful RNAi knockdown was GCGGAUGUCAGAGACUAUGACCACA. Stealth siRNA negative control duplexes with a similar GC content were used as control. C3H10T1/2 stem cells were transfected at 30–50% confluence with siRNA duplexes using Lipofectamine RNAi MAX according to the manufacturer's instructions (Invitrogen).

F-actin Staining—C3H10T1/2 cells were plated on coverslips and treated as described above; 2-day post-confluent cells were washed three times with PBS and fixed in 4% (w/v) formaldehyde for 10 min at room temperature. F-actin was stained with TRITC-conjugated phalloidin (Molecular Probes,

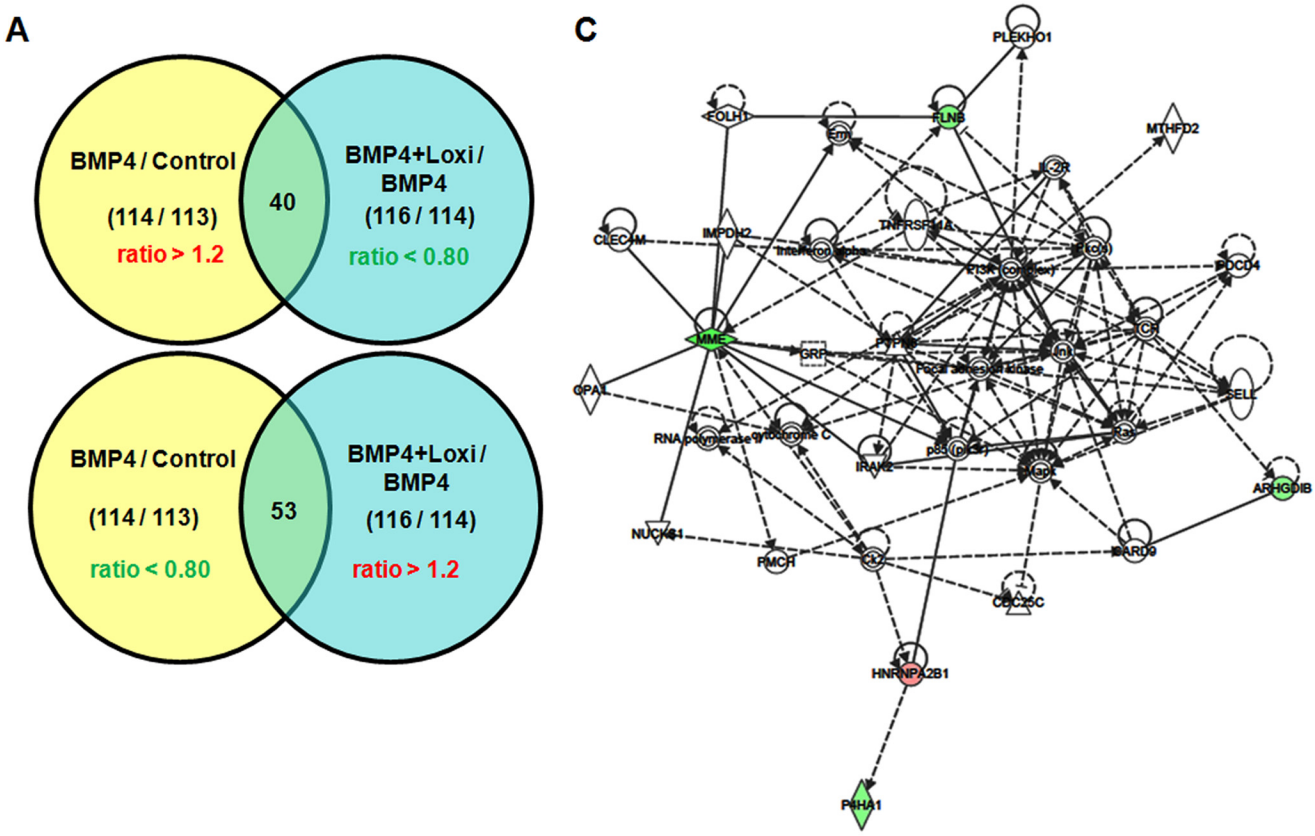

B

	ID	Molecules in Network	Score	Focus Molec	Top Functions
☐	1	↑ALDH2, ↓ANXA3, ↓ANXA5, ATPase, caspase, ↓DDX3X, ↑ENO1, ERK1/2, ↑FKBP9, ↓GAPDH, ↑GOT2, ↑HIST1H1C, ↑HIST1H1E, ↓HNRNPH1, ↓HNRNPM, Hsp70, HSP, ↑HSP90B1, ↓HSPA8, ↓HSPA9, ↑HSPD1, ↓LMNA, ↓MDH2, ↓NPM1, ↑OTUB1, ↓PAK2, peptidylprolyl isomerase, PPI, ↓PPIA, ↑PPIC, ↓PRDX5, ↑PSMC1, Ubiquitin, ↓VCP, ↑YWHAQ	61	27	Hematological Disease, Immunological Disease, Inflammatory Disease
☐	2	60S ribosomal subunit, Actin, Akt, Alpha tubulin, ↓ANXA2, Beta Tubulin, calpain, ↓CCT2, ↓CCT3, ↓CNN2, Collagen type I, ↑COPA, Cyclin E, ↑DCLK1, F Actin, ↓GPI, ↓HNRNPC, Immunoglobulin, ↑IPO5, ↓NME2, ↑PDIA6, ↓PSAP, ↓RPL14, ↑RPL23, ↑RPL7A, ↑RTN4, ↑S100A10, ↓SPTBN1, ↓TLN1, ↓TMOD3, ↓Tpm1, ↓TPT1, Tropomyosin, ↓TUBA1B, ↓UBA1	53	24	Cell Cycle, Cellular Movement, Hematological System Development and Function
☐	3	↑CKAP4, ↓CLIC1, ↓CTSA, DMXL2, DPY30, ↓GNS, ↑HIST1H2BJ/HIST1H2BK, ↑HP1BP3, JMY, KDM6A, ↓KPNB1, LDHAL6B, ↑MATR3, MTHFD2, ↓MYL6, NME3, NUP54, PAGR1, PARP14, PRG2, RIOK2, ↑Rpl10, ↓RPS12, ↑SCPEP1, ↑SNX2, SNX32, SRP19, SUCLA2, ↑SUCLG1, SUMF1, ↓TAGLN2, ↑TPI1, tretinoin, UBC, ZNF184	31	16	Cellular Growth and Proliferation, Lipid Metabolism, Nucleic Acid Metabolism
☐	4	↓ACTN4, ADCY, Ap1, ↑ATP2A2, ↑CAPG, ↓CBR1, CD3, Cg, Creb, ↓Eef1a1, ERK, estrogen receptor, ↑GAS1, ↓HBB, Hsp90, ↑HSPG2, Ikb, IL1, IL12 (complex), LDL, Mek, ↓MIF, Mmp, ↑MT-CO2, NFkB (complex), P38 MAPK, ↓PEBP1, Rnr, ↓RPS12, ↓RPS19, ↓S100A4, Sos, trypsin, ↓TXN, Vegf	28	15	Cellular Movement, Hematological System Development and Function, Immune Cell Trafficking
☐	5	26s Proteasome, ↑ACAA2, CASP1, CCND2, CDT1, CENPA, COL3A1, dihydrotestosterone, EIF4EBP1, ERBB2, ↓G6pd2, GHR, glutathione, ↓GPI, HERC3, Hsp27, KLK3, MAPK8IP1, ↓MIF, ↓MME, NDRG1, NF2, Nos, PRKAA, PSMC3, PSMD8, RNF41, RPGRIP1L, ↑Rps28, SKP2, SNAI2, ↓TALDO1, USP14, ZEB1, ZWINT	11	7	Cellular Development, Cellular Growth and Proliferation, Tumor Morphology
☐	6	↓ARHGDIB, CARD9, CDC25C, Ck2, CLEC4M, cytochrome C, Erm, ↓FLNB, Focal adhesion kinase, FOLH1, GRP, ↑HNRNPA2B1, IL-2R, IMPDH2, Interferon alpha, IRAK2, Jnk, Mapk, ↓MME, MTHFD2, NUCKS1, OPA1, ↓P4HA1, p85 (pik3r), PDCD4, PI3K (complex), Pkc(s), PLEKHO1, PMCH, PTPN6, Ras, RNA polymerase II, SELL, TCR, TNFRSF11A	7	5	Cellular Movement, Organ Morphology, Skeletal and Muscular System Development and Function

FIGURE 1. **Pathway analysis of differentially expressed proteins identified by iTRAQ.** *A,* Venn diagram illustrating the overlap of proteins identified by iTRAQ. *B,* predominant canonical pathways of differentially expressed proteins established by ingenuity pathway analysis. *C,* gene network involved in skeletal and muscular system development. *Red* gene symbols indicate up-regulation and *green* indicate down-regulation in BMP4-treated cells; the remaining genes were not affected (*white*).

Eugene OR) for 30 min at room temperature. Nuclei were counterstained with DAPI. Images were captured with a Leica confocal microscope.

GST-PAK-PBD Binding Assays—The activation of Rac1 (Rac1-GTP) was determined by a pulldown assay using a commercially available kit according to the manufacturers' instructions (Cytoskeleton). Briefly, 2-day post-confluent C3H10T1/2 cells were washed with ice-cold PBS and lysed. The lysates were clarified by centrifugation at 10,000 × *g* at 4 °C for 1 min and incubated with GST-PAK-PBD-agarose beads at 4 °C for 1 h. The beads were washed and eluted. To detect GTP-bound Rac1, eluted agarose-bound proteins were separated by SDS-

TABLE 1

Proteins up-regulated in BMP4-treated cells and down-regulated in those cells when Lox is knocked down

iTRAQ was used to compare protein expression profiles among MSC controls, MSCs treated with BMP4 only and MSCs treated with BMP4 and Lox RNAi. The change cut-off was set at 1.2-fold for all iTRAQ ratios: the ratios >1.2 and <0.80 were used to classify proteins as up- or down-regulated, respectively. Forty proteins were identified as upregulated in BMP4-treated cells and down-regulated when LOX was knocked down.

NCBI accession No.	Protein name	BMP4/control (114/113)	Loxi + BMP4/BMP4 (116/114)
P17182	α-Enolase	2.291	0.692
P63038	60-kDa heat shock protein, mitochondrial	2.679	0.692
P62806	Histone H4	1.995	0.698
Q8CGP1	Histone H2B type 1-K	1.393	0.586
P43274	Histone H1.4	1.225	0.711
Q922R8	Protein-disulfide isomerase A6	1.355	0.698
P08113	Endoplasmin	2.729	0.655
P17751	Triose-phosphate isomerase	1.236	0.731
Q8BMK4	Cytoskeleton-associated protein 4	1.318	0.586
P15864	Histone H1.2	1.871	0.794
Q05793	Basement membrane-specific heparan sulfate proteoglycan core protein	1.406	0.787
P62192	26 S Protease regulatory subunit 4	2.911	0.692
Q8BWT1	3-Ketoacyl-CoA thiolase, mitochondrial	2.831	0.711
Q8K310	Matrin-3	12.023	0.614
P68254	Protein θ	1.941	0.685
Q99P72	Reticulon-4	1.393	0.773
Q6ZWV3	60 S ribosomal protein L10	3.076	0.794
O88569	Heterogeneous nuclear ribonucleoproteins A2/B1	1.445	0.655
Q8BKC5	Importin-5	2.291	0.705
P84244	Histone H3.3	1.722	0.711
P30412	Peptidyl-prolyl cis-trans isomerase C	1.542	0.738
P47738	Aldehyde dehydrogenase, mitochondrial	6.546	0.661
Q9JLM8	Serine/threonine-protein kinase DCLK1	2.559	0.387
P62204	Calmodulin	13.804	0.288
O55143	Sarcoplasmic/endoplasmic reticulum calcium ATPase 2	1.514	0.731
P62830	60 S ribosomal protein L23	1.57	0.794
P12970	60 S ribosomal protein L7a	1.77	0.787
P24452	Macrophage-capping protein	1.282	0.625
Q7TQI3	Ubiquitin thioesterase OTUB1	2.489	0.57
Q3TEA8	Heterochromatin protein 1-binding protein 3	3.105	0.766
Q8CIE6	Coatomer subunit α	1.213	0.724
P05202	Aspartate aminotransferase, mitochondrial	1.871	0.457
Q9CWK8	Sorting nexin-2	1.585	0.643
Q9WUM5	Succinyl-CoA ligase (GDP-forming) subunit α, mitochondrial	1.33	0.581
P00405	Cytochrome c oxidase subunit 2	1.514	0.752
P62858	40 S ribosomal protein S28	2.051	0.738
Q9Z247	FK506-binding protein 9	1.754	0.597
P08207	Protein S100-A10	1.941	0.718
Q01721	Growth arrest-specific protein 1	2.399	0.586
Q920A5	Retinoid-inducible serine carboxypeptidase	2.291	0.429

PAGE, and Western blotting was performed using the antibody against Rac1.

Sample Preparation and iTRAQ Labeling—Total protein was extracted from C3H10T1/2 cells (control, BMP4-treated and LOX knockdown cells) on day 0 using lysis buffer (8 M urea, 2 M thiourea, 2% CHAPS, 60 mM DTT) containing complete protease inhibitor mixture (Roche Applied Science). A total of 100 μg of protein from each group was precipitated overnight with 6 volumes of acetone at 4 °C and the pellets were resuspended in dissolution buffer containing 20 μl of 500 mM triethylammonium bicarbonate and 1 μl of 2% SDS. Subsequently, the resuspended proteins were reduced with 2 μl of 50 mM tris-2-(carboxyethyl)phosphine at 60 °C for 1 h and then alkylated with 1 μl of 200 mM methyl methanethiosulfonate in isopropyl alcohol at room temperature for 10 min, followed by digestion with 10 μg of sequencing grade trypsin (Applied Biosystems) for 16 h at 37 °C. Peptide samples were labeled with iTRAQ tags (isobaric tags for relative and absolute quantitation) at room temperature for 1 h as follows: iTRAQ113 for control C3H10T1/2 cells, iTRAQ114 for BMP4-treated cells, and iTRAQ116 for LOX knockdown cells. Then all the labeled peptides were dried and analyzed by reverse-phase liquid chromatography followed by tandem mass spectrometry (LC-MS/MS).

Statistical Analysis—Values are expressed as mean ± S.D. of at least three independent experiments. The p values were determined by Student's t test, with $p < 0.05$ considered significant.

RESULTS

Proteomics Profiling Identified RhoGDIβ as a Muscular Development-related Protein—A newly developed iTRAQ technique was used to compare protein expression profiles among control C3H10T1/2 cells, C3H10T1/2 cells treated with BMP4, and *Lox* knockdown cells treated with BMP4. We took the cut-offs for all iTRAQ ratios as 1.2-fold changes, that is, ratios of >1.2 or <0.80, to classify proteins as up- or down-regulated, respectively. We were interested in proteins down-regulated by BMP4 that were elevated when *Lox* was knocked down, and proteins up-regulated by BMP4 that were down-regulated by knockdown of *Lox*. According to these criteria, 93 differentially expressed proteins were screened from the iTRAQ experiments (Fig. 1*A*). Forty were up-regulated in BMP4-treated cells and down-regulated again when *Lox* was knocked down (Table 1). Fifty-three were down-regulated in BMP4-treated cells and elevated by knockdown of *Lox* (Table 2). These differentially expressed proteins were analyzed with

TABLE 2

Proteins are down-regulated in BMP4-treated cells and up-regulated in those cells when Lox is knocked down

Fifty-three proteins were identified as down-regulated in BMP4-treated cells and up-regulated when LOX was knocked down by iTRAQ.

NCBI accession No.	Protein name	BMP4/control (114/113)	Loxi + BMP4/BMP4 (116/114)
P26039	Talin-1	0.631	1.528
Q01853	Transitional endoplasmic reticulum ATPase	0.78	1.445
P48036	Annexin A5	0.673	1.225
P07356	Annexin A2	0.402	1.77
Q80X90	Filamin-B	0.457	1.213
P17742	Peptidyl-prolyl cis-trans isomerase A	0.449	2.208
P38647	Stress-70 protein, mitochondrial	0.78	1.294
P58771	Tropomyosin α1 chain	0.366	1.82
P10126	Elongation factor 1-α1	0.525	1.754
P16858	Glyceraldehyde-3-phosphate dehydrogenase	0.308	2.535
Q9D0E1	Heterogeneous nuclear ribonucleoprotein M	0.614	1.33
P80314	T-complex protein 1 subunit β	0.766	1.33
P63017	Heat shock cognate 71-kDa protein	0.586	1.629
Q02053	Ubiquitin-like modifier-activating enzyme 1	0.466	1.675
P08249	Malate dehydrogenase, mitochondrial	0.347	2.109
Q9Z1Q5	Chloride intracellular channel protein 1	0.281	3.802
P48678	Lamin-A/C	0.53	1.294
Q9WVA4	Transgelin-2	0.402	1.629
Q62261	Spectrin β chain, brain 1	0.299	2.535
P70296	Phosphatidylethanolamine-binding protein 1	0.711	1.542
Q60605	Myosin light polypeptide 6	0.655	1.6
Q61937	Nucleophosmin	0.692	1.722
P99029	Peroxiredoxin-5, mitochondrial	0.479	1.977
P57780	Alpha-actinin-4	0.619	1.432
P34884	Macrophage migration inhibitory factor	0.603	1.306
P70168	Importin subunit β-1	0.488	1.556
Q9JHJ0	Tropomodulin-3	0.497	1.38
Q8BFR4	*N*-Acetylglucosamine-6-sulfatase	0.31	1.542
P07091	Protein S100-A4	0.738	1.629
O35737	Heterogeneous nuclear ribonucleoprotein H	0.402	2.443
Q61207	Sulfated glycoprotein 1	0.619	1.486
Q01768	Nucleoside diphosphate kinase B	0.305	5.346
O35639	Annexin A3	0.466	1.614
P63323	40 S ribosomal protein S12	0.012	87.902
Q08093	Calponin-2	0.711	1.556
Q9CR57	60 S ribosomal protein L14	0.394	10.568
P62991	Ubiquitin	0.711	1.33
P16675	Lysosomal protective protein	0.497	1.38
Q62167	ATP-dependent RNA helicase DDX3X	0.787	2.249
Q61391	Neprilysin	0.244	3.076
P10639	Thioredoxin	0.039	99.083
P80318	T-complex protein 1 subunit γ	0.692	1.406
Q9CZX8	40 S ribosomal protein S19	0.637	1.514
P05213	Tubulin α-1B chain	0.075	23.121
Q9Z204	Heterogeneous nuclear ribonucleoproteins C1/C2	0.619	1.202
Q8CIN4	Serine/threonine-protein kinase PAK 2	0.581	1.259
P06745	Glucose-6-phosphate isomerase	0.247	2.399
Q61599	Rho GDP-dissociation inhibitor 2	0.545	1.923
P02088	Hemoglobin subunit β-1	0.679	1.33
P48758	Carbonyl reductase [NADPH] 1	0.625	1.486
Q60715	Prolyl 4-hydroxylase subunit α-1	0.545	1.629
P97324	Glucose-6-phosphate 1-dehydrogenase 2	0.655	1.472
Q93092	Transaldolase	0.698	4.613

ingenuity pathways analysis software. Detailed information is presented in Fig. 1*B*. This complex gene network consists of six major subnetworks. Five proteins were linked to skeletal and muscular system development and function (Fig. 1, *B* and *C*). Among these muscular development-related proteins, RhoGDIβ (ARHGDIB) was down-regulated in C3H10T1/2 cells treated with BMP4 and selected for further investigation on the basis of its involvement in cytoskeletal rearrangement (32–34).

Down-regulation of RhoGDIβ Is Required for BMP4-induced Adipocyte Lineage Commitment—The expression of RhoGDIβ in BMP4-induced committed preadipocytes was confirmed by Western blotting. In line with the proteomics analysis, total cellular RhoGDIβ protein was decreased in C3H10T1/2 cells treated with BMP4 (Fig. 2*A*). To investigate whether RhoGDIβ is a downstream target of Lox, *Lox* was knocked down using siRNA in C3H10T1/2 cells treated with BMP4. Expression of RhoGDIβ inhibited by BMP4 was recovered when *Lox* was knocked down (Fig. 2*B*). Consistent with the protein level, quantitative RT-PCR also demonstrated that *RhoGDIβ* mRNA expression was down-regulated after BMP4 treatment (Fig. 2*C*). The mRNA level of *RhoGDIβ* inhibited by BMP4 was recovered when Lox was knocked down; the expression of another RhoGDI family member, *RhoGDIγ*, was also decreased by BMP4, and this inhibition was also recovered when Lox was knocked down. The expression of *RhoGDIα* was not affected in both BMP4-treated cells and Lox-knocked down cells (Fig. 2*C*).

To test whether the down-regulation of RhoGDIβ is required for BMP4-induced adipocyte lineage commitment, RhoGDIβ was overexpressed in C3H10T1/2 cells using a retroviral system (MSCV). The expression of RhoGDIβ protein was remarkably increased in RhoGDIβ overexpressing cells than in the control

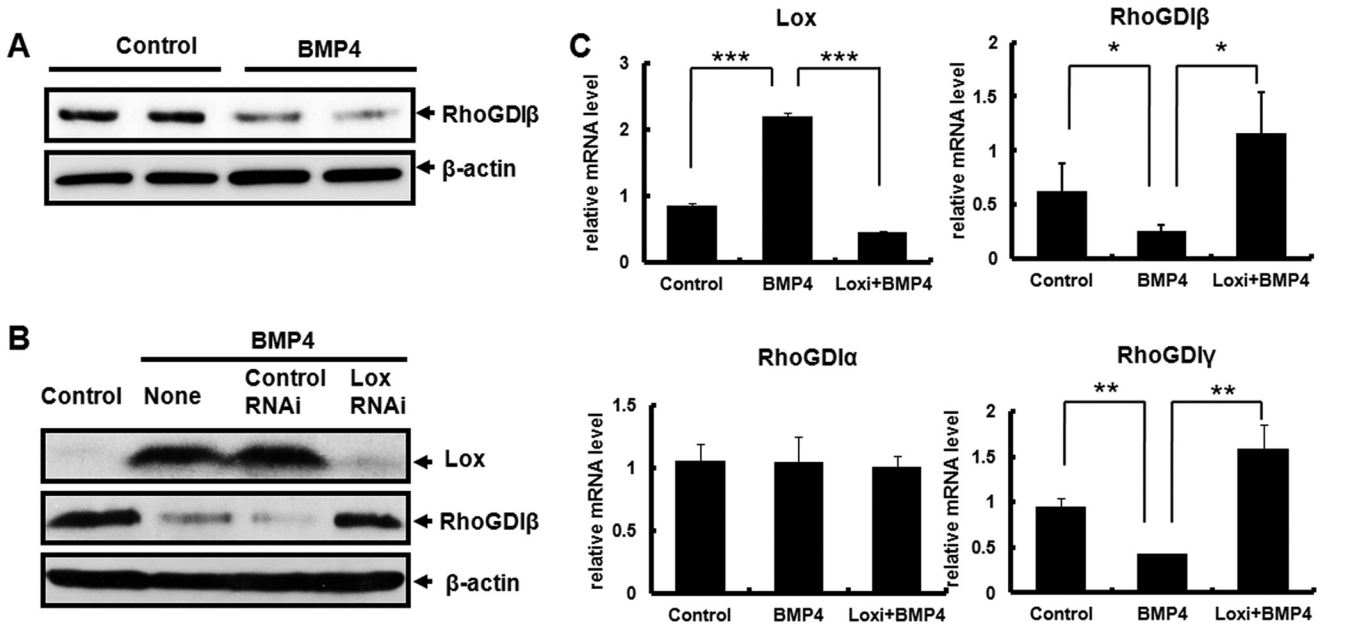

FIGURE 2. **The expression of RhoGDIβ during adipocyte lineage commitment.** C3H10T1/2 cells plated at low density, and treated with or without BMP4 until post-confluence. *A,* the protein level of RhoGDIβ was determined by Western blotting. β-Actin was used as a loading control. *B,* knockdown of Lox expression and its effect on the expression of RhoGDIβ was confirmed by Western blotting. C3H10T1/2 cells were plated at 30% confluence, transfected with *Lox* Stealth RNAi, and 24 h later treated with or without BMP4 until post-confluence. *C*, the mRNA level of *RhoGDIs* was measured by quantitative RT-PCR. Data were obtained from three or more independent experiments and are presented as mean ± S.D. *, $p < 0.05$ compared with the control group or Lox Knockdown group.

cells infected with empty MSCV, as confirmed by Western blotting (Fig. 3*A*). After reaching post-confluence, the cells were given a standard adipocyte differentiation protocol (MDI); this forced expression of RhoGDIβ totally inhibited acquisition of the adipocyte phenotype, as indicated by decreased expression of the adipocyte-specific protein 422/aP2 (Fig. 3*B*) and lower accumulation of cytoplasmic triglyceride staining with Oil Red O (Fig. 3*C*).

RhoGDIβ Inhibits BMP4-induced Adipocyte Lineage Commitment in a Rac1-dependent Manner—RhoGDIβ, an inhibitor of the small G-protein Rho family, prevents activation of Rac1/2, RhoA, and Cdc42. To investigate whether Rac1 mediates the action of RhoGDIβ in adipocyte commitment, we examined the activation of Rac1 during BMP4-induced adipocyte lineage commitment by measuring its binding to the GTPase-binding domain of p21-activated kinase (PAK-PBD) (35). GST-PAK-PBD-bound active Rac1 was detected by Western blotting using the anti-Rac1 antibody. Binding of Rac1 to GST-PAK-PBD was significantly increased after BMP4 treatment (Fig. 4*A*), indicating that Rac1 is significantly activated in BMP4-induced committed preadipocytes. To examine the contribution of RhoGDIβ to BMP4-induced activation of Rac1 further, RhoGDIβ was overexpressed in C3H10T1/2 cells with or without BMP4 treatment, and then the binding of Rac1 to GST-PAK-PBD was examined. Rac1 binding was significantly decreased in RhoGDIβ-overexpressing cells treated with or without BMP4 (Fig. 4*B*). These results demonstrated that the inhibitory effect of RhoGDIβ on BMP4-induced adipocyte commitment is due at least in part to inactivation of Rac1.

Constitutively Active Rac1 Rescues the Inhibition of RhoGDIβ for Adipocyte Lineage Commitment—Because RhoGDIβ inhibits BMP4-induced activation of Rac1 in committed preadi-

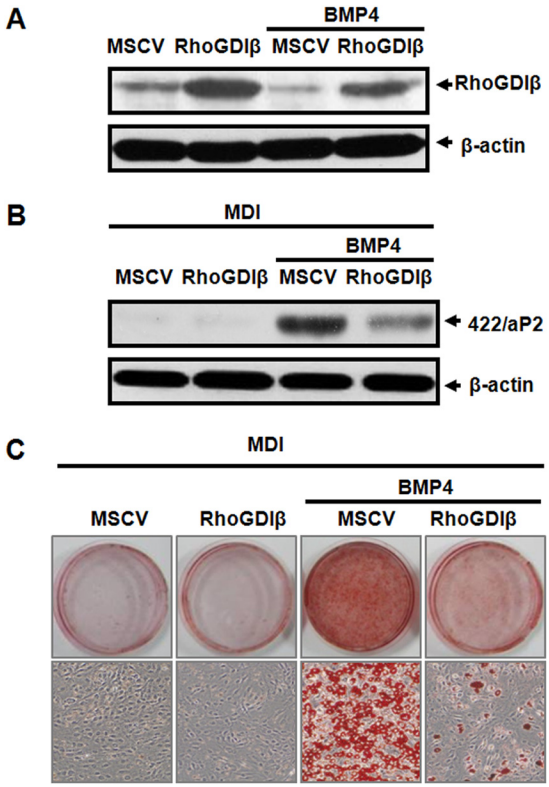

FIGURE 3. **Down-regulation of RhoGDIβ is required for BMP4-induced adipocyte lineage commitment.** C3H10T1/2 cells were infected with retrovirus harboring RhoGDIβ or empty vector, cultured with or without BMP4 until post-confluence, and subjected to the adipocyte differentiation protocol (MDI). *A,* Western blotting of RhoGDIβ expression at post-confluence, β-actin being used as loading control. The effect of RhoGDIβ overexpression on adipocyte lineage commitment and subsequent differentiation was assessed at day 6 by 422/aP2 (*B*) and Oil Red O staining (*C*).

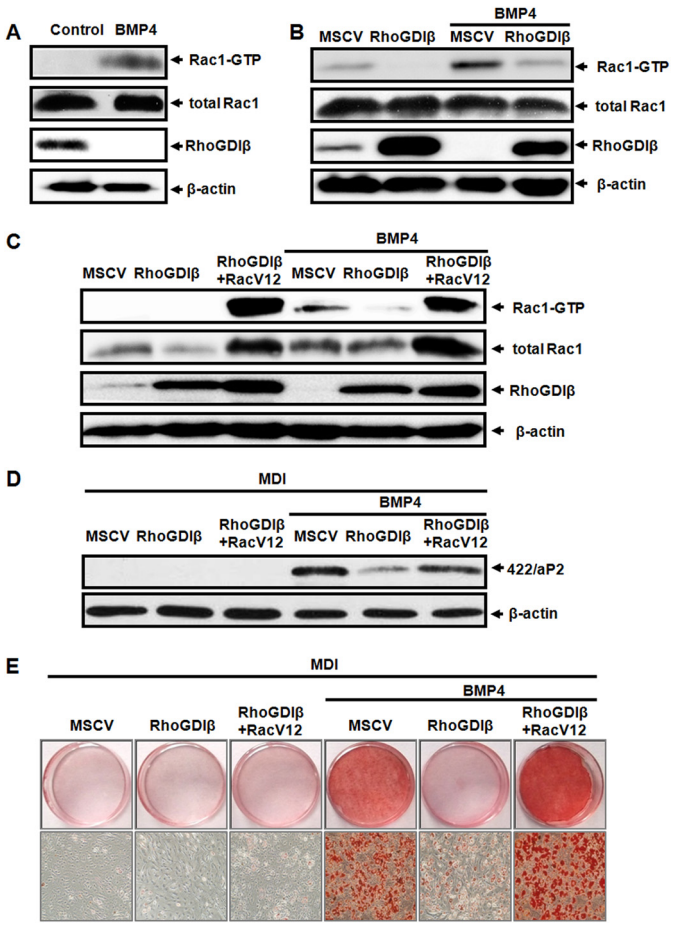

FIGURE 4. **RhoGDIβ blunted BMP4-induced adipocyte lineage commitment via inactivation of Rac1.** C3H10T1/2 cells plated at low density, treated with or without BMP4 until post-confluence. The amount of Rac1 bound to GST-PAK1-PBD fusion protein was measured by Western blotting as described under "Experimental Procedures" (*A*). GST-PAK-PBD-bound active Rac1 was detected in C3H10T1/2 cells infected with retrovirus harboring RhoGDIβ or empty vector, cultured with or without BMP4 until post-confluence (*B*). Active Rac1 was assayed in C3H10T1/2 cells co-overexpressed with RhoGDIβ and RacV12, cultured with or without BMP4 (*C*). RacV12 rescued the adipocyte lineage commitment blocked by RhoGDIβ as assessed by 422/aP2 (*D*) and Oil Red O staining (*E*).

pocytes, we next investigated whether Rac1 could rescue the inhibition of RhoGDIβ for adipocyte lineage commitment. A constitutively active Rac1 mutant (RacV12) and RhoGDIβ were co-overexpressed in C3H10T1/2cells with or without BMP4 treatment. Rac1 binding to GST-PAK-PBD was also examined. As illustrated in Fig. 4*C*, Rac1 activity in C3H10T1/2 cells overexpressing RhoGDIβ with RacV12 was dramatically greater than that in cells overexpressing RhoGDIβ alone. Consistent with these results, this forced expression of RacV12 totally rescued the inhibition of the adipocyte phenotype by RhoGDIβ, as indicated by increased expression of the adipocyte-specific protein 422/aP2 (Fig. 4*D*) and greater accumulation of cytoplasmic triglyceride staining with Oil Red O (Fig. 4*E*). These findings demonstrated that the inhibitory effect of RhoGDIβ on BMP4-induced adipocyte commitment is due to the inactivation of Rac1.

RhoGDIβ Facilitates Smooth Muscle Cell-like Phenotype—C3H10T1/2 cells can undergo commitment and differentiate into multiple mesodermal cell types (14, 36), but inducers of differentiation along one lineage often inhibit differentiation of alternative lineages. For instance, Med23 deficiency facilitates SMC differentiation but represses adipocyte differentiation (20). Because muscle development-related RhoGDIβ suppresses BMP4-induced adipocyte lineage commitment, we speculated that it may favor the commitment to the SMC lineage. To test this hypothesis, C3H10T1/2 cells were infected with MSCV or RhoGDIβ and treated with or without BMP4 until post-confluence, then cultured in SMC differentiation medium for 7 days before the SMC differentiation markers were examined. Quantitative RT-PCR demonstrated that overexpression of RhoGDIβ induced the expression of multiple early and mid smooth muscle cell marker genes, *e.g. Acta2*, *Calponin1*, *Sm22α*, and *Sm22β*, even in the presence of BMP4 (Fig. 5*A*). Furthermore, expression of *smMHC*, a late marker of SMC differentiation, was also significantly induced (Fig. 5*A*). Similarly, Western blotting demonstrated increased protein levels of Calponin1 and Acta2 (Fig. 5*B*) in cells expressing RhoGDIβ, whereas overexpression of constitutively active Rac1 decreased the expression of smooth muscle genes in cells overexpressing RhoGDIβ (Fig. 5). These results demonstrated that RhoGDIβ represses BMP4-induced adipocytic lineage commitment and favors smooth muscle-like cells differentiation.

RhoGDIβ Favors Smooth Muscle-like Cell Fate via Phospho-MLC-dependent Actin Reorganization—In line with our previous studies (15), F-actin filaments in uncommitted post-confluent C3H10T1/2 cells took the form of stress fibers, forming long linear bundles, whereas such F-actin fibers were significantly decreased after BMP4 treatment (Fig. 6*A*). Overexpression of RhoGDIβ almost totally rescued the F-actin stress fibers that were disrupted during adipocyte lineage commitment induced by BMP4 (Fig. 6*B*). In contrast, RhoGDIβ-induced F-actin stress fibers were disrupted again in cells overexpressing RacV12, which became similar in structure to committed preadipocytes induced by BMP4 (Fig. 6*B*). These findings indicated that RhoGDIβ facilitates the smooth muscle cell fate through F-actin reorganization.

Both MLC and cofilin are related to the dynamics of F-actin. MLC, when phosphorylated (Thr^{18}/Ser^{19}), is thought to promote the assembly of filaments (37). Cofilin is a ubiquitous actin-binding factor required for reorganizing actin filaments. Phosphorylation of cofilin at a single site (Ser^{3}) inhibits its actin-depolymerizing activity (38). We therefore examined whether RhoGDIβ affected the phosphorylation of MLC or cofilin. Our results demonstrated that both phospho-MLC (Thr^{18}/Ser^{19}) and phospho-cofilin (Ser^{3}) were lower in BMP4-treated cells than control cells (Fig. 6*C*). We then reasoned that if the decrease in phospho-MLC or phospho-cofilin is a consequence of high levels of active Rac1, then overexpression of RhoGDIβ should reset phospho-cofilin or phospho-MLC to higher levels. Our data demonstrated that overexpression of RhoGDIβ drastically increased the levels of phospho-MLC (Thr^{18}/Ser^{19}) and phospho-cofilin (Ser^{3}) in cells with or without BMP4 treatment (Fig. 6*D*). However, overexpression of constitutively active Rac1 only decreased the amount of phospho-MLC in cells overexpressing RhoGDIβ (Fig. 6*D*), whereas phosphorylated cofilin was not affected. These results indi-

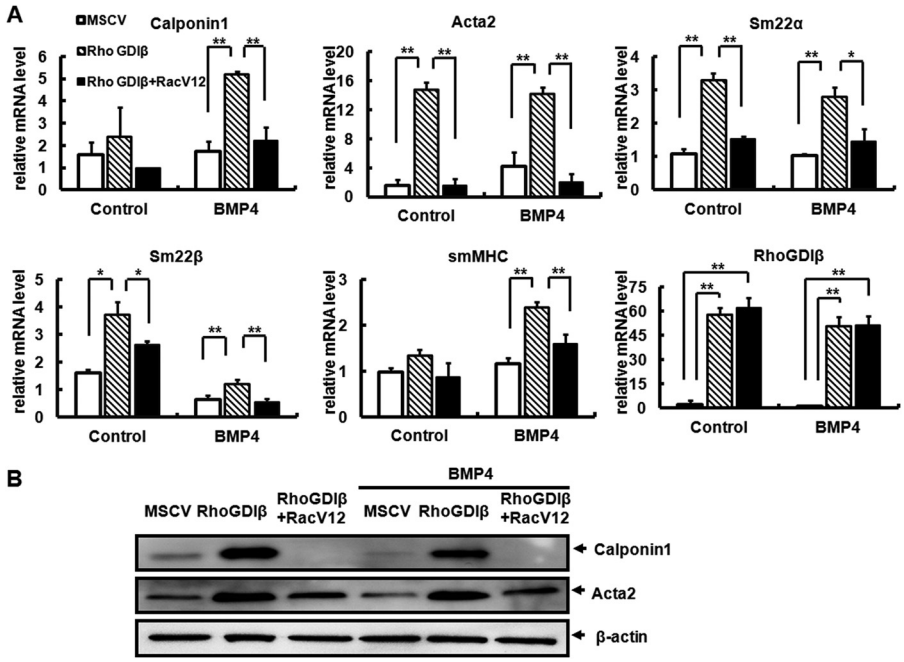

FIGURE 5. **Overexpression of RhoGDIβ promotes smooth muscle-like phenotype.** C3H10T1/2 cells infected with the indicated retrovirus were treated with or without BMP4 until post-confluence and then cultured in SMC differentiation medium for 7 days. Following treatments, the mRNA expression levels of RhoGDIβ and SMC-specific genes were measured using quantitative RT-PCR. Data were obtained from three or more independent experiments and are presented as means ± S.D. *, $p < 0.05$ compared with the control group (*A*). The effect of RacV12 on the protein levels of Calponin1 and Acta2 in cells co-overexpressing RhoGDIβ; β-actin was used as a loading control (*B*).

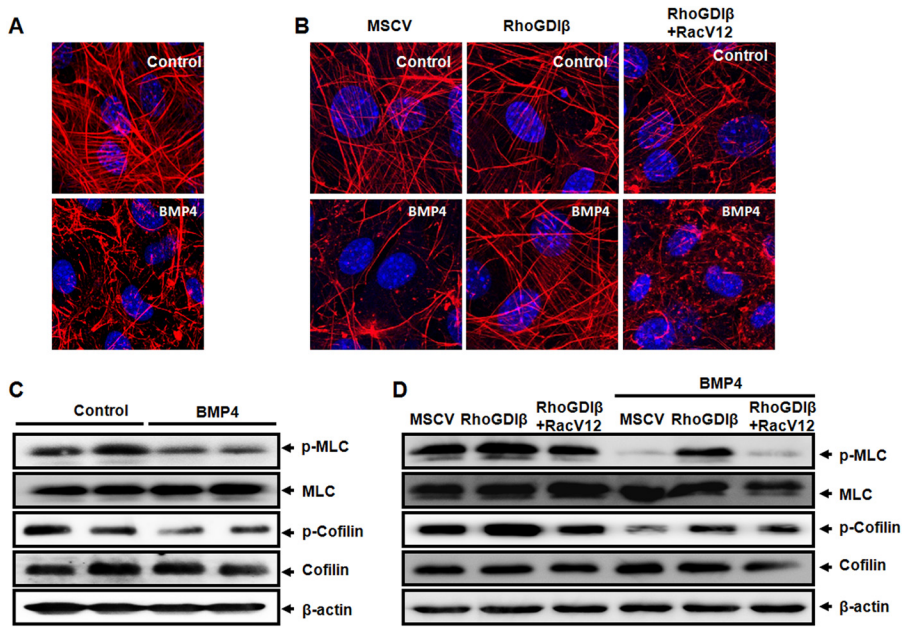

FIGURE 6. **RhoGDIβ favors SM-like cell fate via phospho-MLC-dependent actin reorganization.** C3H10T1/2 cells were plated at 30% confluence and treated with or without BMP4 until post-confluence. *A,* F-actin in the cells with different treatments was stained with rhodamine-conjugated phalloidin and visualized by confocal laser-scanning microscopy. *Bar* = 10 μM. *B,* constitutively active Rac1 disrupted the stress fibers formed by RhoGDIβ overexpression. *Bar* = 10 μM. *C,* BMP4 inhibits the phosphorylation of MLC and cofilin. Phosphorylation of MLC and cofilin was revealed by Western blotting. β-Actin was used as a loading control. *D,* phosphorylation of MLC and cofilin in cells infected with RhoGDIβ or co-infected with RhoGDIβ and RacV12, which were plated at 30% confluence and treated with or without BMP4 until post-confluence. Phosphorylation of MLC and cofilin was revealed by Western blotting.

cated that RhoGDIβ reorganizes F-actin and promotes smooth muscle-like cell lineage commitment by increasing phospho-MLC.

DISCUSSION

MSCs are progenitors capable of differentiating into multiple cell types including adipocytes, osteoblasts, chondrocytes, tenocytes, skeletal myocytes, and visceral stromal cells (39–44). The decision made by a mesenchymal stem cell to commit to a particular lineage is highly context-dependent and involves the integration of multiple extracellular signals to drive the outcome. Our previous findings demonstrated that BMP4 induces nearly complete commitment of C3H10T1/2 cells to the adipocyte lineage (16, 17) and disrupts the formation of filamen-

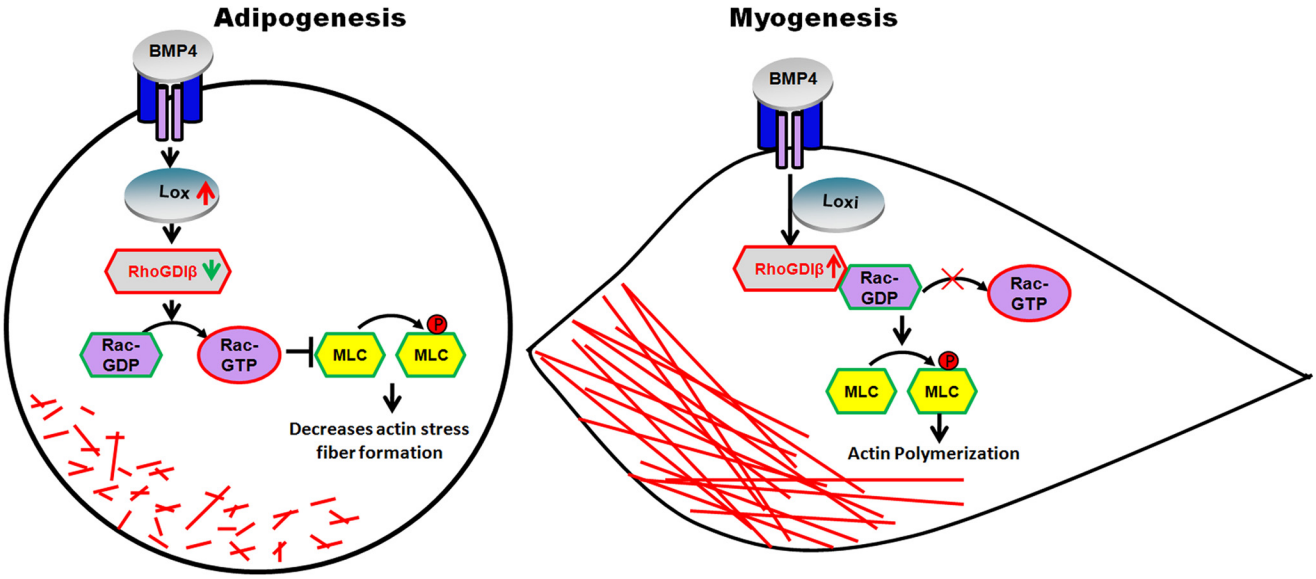

FIGURE 7. **Model of RhoGDIβ-regulated MSC commitment to adipocyte or SMC lineage.** BMP4 signaling increases the expression of Lox, which down-regulates the expression of RhoGDIβ. The enhanced Rac1 activation due to the lowering of RhoGDIβ leads to actin filament disruption by decreasing the phosphorylation of MLC, facilitating adipocyte lineage commitment. Knockdown of Lox prevents BMP4-induced RhoGDIβ down-regulation and Rac1 activation, resulting in enhanced phosphorylation of MLC and formation of stress fibers, which drive commitment to the smooth muscle-like cell lineage.

tous actin (15). Both BMP4-induced adipocyte lineage commitment and actin reorganization are regulated by Lox (15, 16). However, the molecular mechanisms by which Lox regulates the changes in the cytoskeleton are not fully understood. In this study, RhoGDIβ was identified by proteomics profiling as a potential target downstream of the BMP4-Lox signaling axis.

Rho family GTPases are important in many cellular functions (45). RhoGDIs, potent negative regulators of Rho family GTPases, are characterized by their ability to prevent nucleotide exchange and membrane association (31). Within the RhoGDI family members, RhoGDIα is ubiquitously expressed, whereas RhoGDIβ and RhoGDIγ expression is tissue-specific (31). However, a recent report that RhoGDIβ mRNA has a widespread tissue distribution (46) indicates a potential role in other tissues. Accumulating evidence indicates that Rho activity is important for normal muscle development. In this study, we demonstrated the importance of RhoGDIβ in regulating MSCs differentiation into smooth muscle-like cells or adipocytes. We found that RhoGDIβ was down-regulated by BMP4, and inhibition of Lox up-regulated it during adipocyte lineage commitment (Fig. 2). Overexpression of RhoGDIβ completely prevented BMP4-induced adipocyte lineage commitment while simultaneously stimulating smooth muscle-like cell differentiation (Figs. 3 and 5). Thus, RhoGDIβ appears to have opposing roles in adipogenesis and myogenesis. Previous studies by other groups demonstrated that the major Rho inhibitory protein p190-B RhoGAP can also direct the adipogenesis-myogenesis fate decision (47). In contrast, cells that exhibit excessive Rho activity are defective for adipogenesis and undergo myogenesis in response to insulin-like growth factor-1 exposure (47). However, the two studies yielded opposite conclusions about the determination of adipogenesis and myogenesis fates by GTPase inhibitors. This controversy is probably attributable to the different cell models and inducers used.

The commitment of MSCs to different lineages is regulated by many local tissue microenvironmental cues. Cell shape can drive MSC differentiation into different lineages in response to the same soluble factor. Recently, it was reported that cell shape regulates the commitment of human mesenchymal stem cells (hMSCs) to an adipocyte or osteoblast fate (23). Interestingly, a change of cell shape also implements a switch between chondrogenic and smooth muscle cell fates (24), suggesting a common molecular mechanism controlling lineage commitment. It is well established that RhoGTPases regulate cell shape through modulating the cytoskeleton (45). In the present study F-actin reorganization were observed during adipogenenic or myogenenic commitment. F-actin stress fibers were significantly decreased in BMP4-induced committed preadipocytes (15) (Fig. 6, *A* and *B*). The overexpression of RhoGDIβ almost totally rescued the formation of F-actin stress fibers, which were disrupted during BMP4-induced adipocyte lineage commitment (Fig. 6*B*). These findings indicate that RhoGDIβ could regulate adipogenesis *versus* myogenesis via cytoskeletal reorganization.

The small Rho GTPase family members known as Rho, Rac, and Cdc42 were initially linked to changes in the filamentous actin system involving the formation of stress fibers. Because Rho family small GTPases have well established roles in cytoskeletal remodeling, it is not surprising that Rho GTPases are involved in mediating the signals from cytoskeletal changes to determination of cell fate. Rho GTPases cycle between an inactive (GDP bound) state located in the cytosol and an active (GTP bound) state located on the membrane (48). RhoGDIs inhibit Rho GTPases by direct interaction and by maintaining Rho proteins in the inactive state in the cytoplasm and restraining them from the activation site on the membrane (31). A previous study demonstrated that LOX facilitates the formation of the p130 (Cas)/Crk/DOCK180 signaling complex that promotes Rac activation (26). Rac and Cdc42 activity and actin

stress fibers also decreased with the reduction in LOX activity, indicating that Rac activation and actin stress fibers are associated with Lox. This study provides evidence that Rac1 is activated in response to BMP4 treatment, and overexpression of RhoGDIβ (Lox downstream target) prevents BMP4-induced activation of Rac1 and related cytoskeletal reorganization and adipocyte lineage commitment (Figs. 3, 4, and 6), simultaneously promoting smooth muscle-like cell commitment (Fig. 5). Moreover, forced expression of RacV12 totally rescued the inhibition of the adipocyte phenotype by RhoGDIβ and disrupted the stress fibers in cells overexpressing RhoGDIβ (Figs. 4, *C–E,* and 6), simultaneously preventing the formation of the smooth muscle-like phenotype (Fig. 5). Because RhoGDIs are thought to be common inhibitors of all Rho family functions, it is possible that Rho and Cdc42 also contribute to RhoGDIβ-mediated cell fate determination.

In summary, we have identified a novel role of RhoGDIβ in regulating smooth muscle-like cell and adipocyte fate determination. Down-regulation of RhoGDIβ by the BMP4-Lox signaling axis is required for Rac1-mediated disruption of filamentous actin and adipocyte lineage commitment. Overexpression of RhoGDIβ inhibits the BMP4-induced activation of Rac1, resulting in the formation of stress fibers and smooth muscle-like commitment by increasing phospho-MLC (Fig. 7). Our results suggest a novel role of RhoGDIβ linking adipogenesis and myogenesis.

Acknowledgment—We acknowledge Dr. Debbie Thurmond for the supply of Rac1 constructs.

REFERENCES

1. Bjorntorp, P. (1974) Size, number and function of adipose tissue cells in human obesity. *Horm. Metab. Res.* **4,** 77–83
2. Faust, I. M., Johnson, P. R., Stern, J. S., and Hirsch, J. (1978) Diet-induced adipocyte number increase in adult rats: a new model of obesity. *Am. J. Physiol.* **235,** E279–E286
3. Johnson, P. R., Stern, J. S., Greenwood, M. R., and Hirsch, J. (1978) Adipose tissue hyperplasia and hyperinsulinemia on Zucker obese female rats: a developmental study. *Metabolism* **27,** 1941–1954
4. Bays, H. E., González-Campoy, J. M., Bray, G. A., Kitabchi, A. E., Bergman, D. A., Schorr, A. B., Rodbard, H. W., and Henry, R. R. (2008) Pathogenic potential of adipose tissue and metabolic consequences of adipocyte hypertrophy and increased visceral adiposity. *Expert Rev. Cardiovasc. Ther.* **6,** 343–368
5. Gupta, R. K., Mepani, R. J., Kleiner, S., Lo, J. C., Khandekar, M. J., Cohen, P., Frontini, A., Bhowmick, D. C., Ye, L., Cinti, S., and Spiegelman, B. M. (2012) Zfp423 expression identifies committed preadipocytes and localizes to adipose endothelial and perivascular cells. *Cell Metab.* **15,** 230–239
6. Rodeheffer, M. S., Birsoy, K., and Friedman, J. M. (2008) Identification of white adipocyte progenitor cells *in vivo*. *Cell* **135,** 240–249
7. Tran, K. V., Gealekman, O., Frontini, A., Zingaretti, M. C., Morroni, M., Giordano, A., Smorlesi, A., Perugini, J., De Matteis, R., Sbarbati, A., Corvera, S., and Cinti, S. (2012) The vascular endothelium of the adipose tissue gives rise to both white and brown fat cells. *Cell Metab.* **15,** 222–229
8. Wang, Q. A., Tao, C., Gupta, R. K., and Scherer, P. E. (2013) Tracking adipogenesis during white adipose tissue development, expansion and regeneration. *Nat. Med.* **19,** 1338–1344
9. Yu, Z. K., Wright, J. T., and Hausman, G. J. (1997) Preadipocyte recruitment in stromal vascular cultures after depletion of committed preadipocytes by immunocytotoxicity. *Obes. Res.* **5,** 9–15
10. Caplan, A. I. (1991) Mesenchymal stem cells. *J. Orthop. Res.* **9,** 641–650
11. Caplan, A. I. (1994) The mesengenic process. *Clin. Plast. Surg.* **21,** 429–435
12. Young, H. E., Mancini, M. L., Wright, R. P., Smith, J. C., Black, A. C., Jr., Reagan, C. R., and Lucas, P. A. (1995) Mesenchymal stem-cells reside within the connective tissues of many organs. *Dev. Dyn.* **202,** 137–144
13. Reznikoff, C. A., Brankow, D. W., and Heidelberger, C. (1973) Establishment and characterization of a cloned line of C3H mouse embryo cells sensitive to post-confluence inhibition of division. *Cancer Res.* **33,** 3231–3238
14. Taylor, S. M., and Jones, P. A. (1979) Multiple new phenotypes induced in 10T1/2 and 3T3 cells treated with 5-azacytidine. *Cell* **17,** 771–779
15. Huang, H. Y., Hu, L. L., Song, T. J., Li, X., He, Q., Sun, X., Li, Y. M., Lu, H. J., Yang, P. Y., and Tang, Q. Q. (2011) Involvement of cytoskeleton-associated proteins in the commitment of C3H10T1/2 pluripotent stem cells to adipocyte lineage induced by BMP2/4. *Mol. Cell. Proteomics* **10,** 10.1074/mcp.M110.002691
16. Huang, H., Song, T. J., Li, X., Hu, L., He, Q., Liu, M., Lane, M. D., and Tang, Q. Q. (2009) BMP signaling pathway is required for commitment of C3H10T1/2 pluripotent stem cells to the adipocyte lineage. *Proc. Natl. Acad. Sci. U.S.A.* **106,** 12670–12675
17. Tang, Q. Q., Otto, T. C., and Lane, M. D. (2004) Commitment of C3H10T1/2 pluripotent stem cells to the adipocyte lineage. *Proc. Natl. Acad. Sci. U.S.A.* **101,** 9607–9611
18. Huang, H. Y., Chen, S. Z., Zhang, W. T., Wang, S. S., Liu, Y., Li, X., Sun, X., Li, Y. M., Wen, B., Lei, Q. Y., and Tang, Q. Q. (2013) Induction of EMT-like response by BMP4 via up-regulation of lysyl oxidase is required for adipocyte lineage commitment. *Stem Cell Res.* **10,** 278–287
19. Hirschi, K. K., Rohovsky, S. A., and D'Amore, P. A. (1998) PDGF, TGF-β, and heterotypic cell-cell interactions mediate endothelial cell-induced recruitment of 10T1/2 cells and their differentiation to a smooth muscle fate. *J. Cell Biol.* **141,** 805–814
20. Yin, J. W., Liang, Y., Park, J. Y., Chen, D., Yao, X., Xiao, Q., Liu, Z., Jiang, B., Fu, Y., Bao, M., Huang, Y., Liu, Y., Yan, J., Zhu, M. S., Yang, Z., Gao, P., Tian, B., Li, D., and Wang, G. (2012) Mediator MED23 plays opposing roles in directing smooth muscle cell and adipocyte differentiation. *Genes Dev.* **26,** 2192–2205
21. Wang, S. S., Huang, H. Y., Chen, S. Z., Li, X., Liu, Y., Zhang, W. T., and Tang, Q. Q. (2013) Early growth response 2 (Egr2) plays opposing roles in committing C3H10T1/2 stem cells to adipocytes and smooth muscle-like cells. *Int. J. Biochem. Cell Biol.* **45,** 1825–1832
22. Long, J. Z., Svensson, K. J., Tsai, L., Zeng, X., Roh, H. C., Kong, X., Rao, R. R., Lou, J., Lokurkar, I., Baur, W., Castellot, J. J., Jr., Rosen, E. D., and Spiegelman, B. M. (2014) A smooth muscle-like origin for beige adipocytes. *Cell Metab.* **19,** 810–820
23. McBeath, R., Pirone, D. M., Nelson, C. M., Bhadriraju, K., and Chen, C. S. (2004) Cell shape, cytoskeletal tension, and RhoA regulate stem cell lineage commitment. *Dev. Cell* **6,** 483–495
24. Gao, L., McBeath, R., and Chen, C. S. (2010) Stem cell shape regulates a chondrogenic versus myogenic fate through Rac1 and N-cadherin. *Stem Cells* **28,** 564–572
25. Mack, C. P., Somlyo, A. V., Hautmann, M., Somlyo, A. P., and Owens, G. K. (2001) Smooth muscle differentiation marker gene expression is regulated by RhoA-mediated actin polymerization. *J. Biol. Chem.* **276,** 341–347
26. Payne, S. L., Hendrix, M. J., and Kirschmann, D. A. (2006) Lysyl oxidase regulates actin filament formation through the p130(Cas)/Crk/DOCK180 signaling complex. *J. Cell. Biochem.* **98,** 827–837
27. Ridley, A. J., and Hall, A. (1992) The small GTP-binding protein rho regulates the assembly of focal adhesions and actin stress fibers in response to growth factors. *Cell* **70,** 389–399
28. Ridley, A. J., Paterson, H. F., Johnston, C. L., Diekmann, D., and Hall, A. (1992) The small GTP-binding protein rac regulates growth factor-induced membrane ruffling. *Cell* **70,** 401–410
29. Nobes, C. D., and Hall, A. (1995) Rho, rac, and cdc42 GTPases regulate the assembly of multimolecular focal complexes associated with actin stress fibers, lamellipodia, and filopodia. *Cell* **81,** 53–62
30. Hall, A. (2012) Rho family GTPases. *Biochem. Soc. Trans.* **40,** 1378–1382
31. Dovas, A., and Couchman, J. R. (2005) RhoGDI: multiple functions in the regulation of Rho family GTPase activities. *Biochem. J.* **390,** 1–9

32. Abramovici, H., Mojtabaie, P., Parks, R. J., Zhong, X. P., Koretzky, G. A., Topham, M. K., and Gee, S. H. (2009) Diacylglycerol kinase ζ regulates actin cytoskeleton reorganization through dissociation of Rac1 from RhoGDI. *Mol. Biol. Cell* **20,** 2049–2059
33. Sun, J., and Barbieri, J. T. (2004) ExoS Rho GTPase-activating protein activity stimulates reorganization of the actin cytoskeleton through Rho GTPase guanine nucleotide disassociation inhibitor. *J. Biol. Chem.* **279,** 42936–42944
34. Rivero, F., Illenberger, D., Somesh, B. P., Dislich, H., Adam, N., and Meyer, A. K. (2002) Defects in cytokinesis, actin reorganization and the contractile vacuole in cells deficient in RhoGDI. *EMBO J.* **21,** 4539–4549
35. Bagrodia, S., Taylor, S. J., Creasy, C. L., Chernoff, J., and Cerione, R. A. (1995) Identification of a mouse p21Cdc42/Rac activated kinase. *J. Biol. Chem.* **270,** 22731–22737
36. Pinney, D. F., and Emerson, C. P., Jr. (1989) 10T1/2 cells: an in vitro model for molecular genetic analysis of mesodermal determination and differentiation. *Environ. Health Perspect.* **80,** 221–227
37. Chen, B. H., Tzen, J. T., Bresnick, A. R., and Chen, H. C. (2002) Roles of Rho-associated kinase and myosin light chain kinase in morphological and migratory defects of focal adhesion kinase-null cells. *J. Biol. Chem.* **277,** 33857–33863
38. Kuhn, T. B., Meberg, P. J., Brown, M. D., Bernstein, B. W., Minamide, L. S., Jensen, J. R., Okada, K., Soda, E. A., and Bamburg, J. R. (2000) Regulating actin dynamics in neuronal growth cones by ADF/cofilin and rho family GTPases. *J. Neurobiol.* **44,** 126–144
39. Gronthos, S., Zannettino, A. C., Hay, S. J., Shi, S., Graves, S. E., Kortesidis, A., and Simmons, P. J. (2003) Molecular and cellular characterisation of highly purified stromal stem cells derived from human bone marrow. *J. Cell Sci.* **116,** 1827–1835
40. Pittenger, M. F., Mackay, A. M., Beck, S. C., Jaiswal, R. K., Douglas, R., Mosca, J. D., Moorman, M. A., Simonetti, D. W., Craig, S., and Marshak, D. R. (1999) Multilineage potential of adult human mesenchymal stem cells. *Science* **284,** 143–147
41. Smith, J. R., Pochampally, R., Perry, A., Hsu, S. C., and Prockop, D. J. (2004) Isolation of a highly clonogenic and multipotential subfraction of adult stem cells from bone marrow stroma. *Stem Cells* **22,** 823–831
42. Horwitz, E. M., Prockop, D. J., Fitzpatrick, L. A., Koo, W. W., Gordon, P. L., Neel, M., Sussman, M., Orchard, P., Marx, J. C., Pyeritz, R. E., and Brenner, M. K. (1999) Transplantability and therapeutic effects of bone marrow-derived mesenchymal cells in children with osteogenesis imperfecta. *Nat. Med.* **5,** 309–313
43. Pereira, R. F., Halford, K. W., O'Hara, M. D., Leeper, D. B., Sokolov, B. P., Pollard, M. D., Bagasra, O., and Prockop, D. J. (1995) Cultured adherent cells from marrow can serve as long-lasting precursor cells for bone, cartilage, and lung in irradiated mice. *Proc. Natl. Acad. Sci. U.S.A.* **92,** 4857–4861
44. Jiang, Y., Jahagirdar, B. N., Reinhardt, R. L., Schwartz, R. E., Keene, C. D., Ortiz-Gonzalez, X. R., Reyes, M., Lenvik, T., Lund, T., Blackstad, M., Du, J., Aldrich, S., Lisberg, A., Low, W. C., Largaespada, D. A., and Verfaillie, C. M. (2002) Pluripotency of mesenchymal stem cells derived from adult marrow. *Nature* **418,** 41–49
45. Etienne-Manneville, S., and Hall, A. (2002) Rho GTPases in cell biology. *Nature* **420,** 629–635
46. Theodorescu, D., Sapinoso, L. M., Conaway, M. R., Oxford, G., Hampton, G. M., and Frierson, H. F., Jr. (2004) Reduced expression of metastasis suppressor RhoGDI2 is associated with decreased survival for patients with bladder cancer. *Clin. Cancer Res.* **10,** 3800–3806
47. Sordella, R., Jiang, W., Chen, G. C., Curto, M., and Settleman, J. (2003) Modulation of Rho GTPase signaling regulates a switch between adipogenesis and myogenesis. *Cell* **113,** 147–158
48. Jaffe, A. B., and Hall, A. (2005) Rho GTPases: biochemistry and biology. *Annu. Rev. Cell Dev. Biol.* **21,** 247–269